Adiabatic heuristic principle on a torus and generalized Streda formula

Koji Kudo[1] and Yasuhiro Hatsugai[1,2]
[1]*Graduate School of Pure and Applied Sciences, University of Tsukuba, Tsukuba, Ibaraki 305-8571, Japan*
[2]*Department of Physics, University of Tsukuba, Tsukuba, Ibaraki 305-8571, Japan*

(Received 7 April 2020; revised 6 August 2020; accepted 14 August 2020; published 8 September 2020)

Although the adiabatic heuristic argument of the fractional quantum Hall states has been successful, continuous modification of the statistics of anyons is strictly prohibited due to algebraic constraints of the braid group on a torus. We have numerically shown that the adiabatic heuristic principle for anyons is still valid even though the Hamiltonians cannot be modified continuously. The Chern number of the ground-state multiplet is the adiabatic invariant, while the number of the topological degeneracy behaves wildly. A generalized Streda formula is proposed that explains the degeneracy pattern. Nambu-Goldstone modes associated with the anyon superconductivity are also suggested numerically.

DOI: 10.1103/PhysRevB.102.125108

I. INTRODUCTION

Over the past decade, topology has come to the fore in modern condensed-matter physics. The quantum Hall (QH) effect [1,2] is a prime example of topologically nontrivial phases, where the quantized Hall conductance is given by the Chern number [3–6]. Topological concepts enrich material phases beyond the Ginzburg-Landau theory. The fractional QH (FQH) state [7] is a typical example of the quantum liquid with topological order [8]. It hosts fractionalized excitations that carry fractional charges and fractional statistics [9–11], which is the hallmark of topologically ordered phases [12]. The topological degeneracy is closely related to these fractionalizations [8,13–15]. Some of the non-Abelian topological order can be used for a possible quantum computation [16–20].

Point particles in two dimensions can be charge-flux composites associated with a singular gauge transformation [21]. In relation to the composite fermion picture [22,23], the flux attachment has been quite successful at describing the FQH effect; the FQH effect at filling factor $\nu = p/(2mp \pm 1)$, with p and m being integers, can be understood as the $\nu = p$ integer QH (IQH) effect of the composite fermions. This concept is further developed to the "adiabatic heuristic principle" [24,25]. It states that both states are adiabatically connected through intermediate systems of anyons. This characterization of the QH states based on the adiabatic deformation is a typical example of the topological classification as is widely applied to recent studies of topological phases.

We note that a careful setup is required to carry the program of this adiabatic heuristic principle for concrete systems. The statistical phase θ of anyons is governed by a representation of the fundamental group of the many-particle configuration space (braid group) [26]. Therefore, the world lines of the system needs to satisfy the braid group constraint.

As for topological phenomena, the geometry of the system is crucially important. With boundaries, low-energy modes appear as edge states even for gapped systems. Thus, for the demonstration of the adiabatic heuristic principle, the torus geometry without any boundaries is favorable [27]. However, an algebraic constraint of the braid group on a torus [13,28–32] prohibits continuous change in the statistical phase θ. This makes it impossible to apply the adiabatic heuristic principle naively.

In this paper, we show that the adiabatic heuristic principle indeed remains valid on a torus. Here, "adiabatic" is used in the sense that the gap remains open, although continuous deformation of the Hamiltonian is impossible. The many-body Chern number of the ground-state multiplet is also calculated numerically, which serves as the adiabatic invariant while the topological degeneracy changes wildly. We propose a generalized Streda formula to characterize the obtained degeneracy pattern in relation to the Chern number, which follows from the translational invariance of anyons. At the gap closing point, the Chern number changes sign, and anyon superconductivity [37–39] is expected.

II. ADIABATIC HEURISTIC PRINCIPLE AND BRAID GROUP

Let us here briefly derive the fundamental relation of the adiabatic heuristic principle [24,25]. We consider a QH system of N_a particles with charge $-e$ in a uniform magnetic field. According to the adiabatic heuristic principle, the QH state is adiabatically deformed by trading the external fluxes for the statistical ones of anyons. Since the total flux remains constant ($N_\phi + N_a\theta/\pi = \text{const}$), one has the relation $1/\nu + \theta/\pi = \text{const}$, where N_ϕ is the number of external fluxes, θ is the statistics of anyons, and $\nu = N_a/N_\phi$. Assuming that the $\nu = p$ IQH state of fermions ($\theta = \pi$) is included in this series, one has $\nu = p/[p(1 - \theta/\pi) + 1]$.

From the analysis of the braid group on a torus [13,28–32], the relation $1/\nu + \theta/\pi = \text{const}$ is rederived (see Appendix A) with an *additional* constraint, as explained below. The

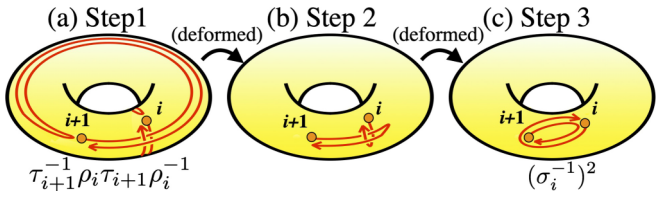

FIG. 1. Pictorial proof of Eq. (1) [28]. (a) The paths of the four moving processes ρ_i^{-1}, τ_{i+1}, ρ_i, and τ_{i+1}^{-1} are presented from bottom to top. (c) The path in (a) can be deformed into that in (c) through that in (b).

generators of the braid group on a torus are denoted as σ_i, τ_i and ρ_i, where σ_i $(i = 1, \ldots, N_a - 1)$ is a local exchange between the ith and $(i+1)$th anyons and τ_i and ρ_i $(i = 1, \ldots, N_a)$ are global moves of the ith anyon along a non-contractible loop on the torus in the x and y directions. Now, we take the basis $|\{\boldsymbol{r}_k\}; w\rangle$ for its expressions, where $\{\boldsymbol{r}_k\}$ is the position of anyons and $w = 1, \ldots, M$ is the extra internal index that is necessary to satisfy the braid group constraints on a torus, as seen below. We assume that anyons are Abelian: $\sigma_i = e^{i\theta}\mathbf{1}_M$, where $\mathbf{1}_M$ is the M-dimensional unit matrix. As shown in Fig. 1 [28], the generators σ_i, τ_i, and ρ_i need to satisfy

$$\tau_{i+1}^{-1}\rho_i\tau_{i+1}\rho_i^{-1} = (\sigma_i^{-1})^2 = e^{-i2\theta}\mathbf{1}_M. \tag{1}$$

By taking a determinant of Eq. (1), we have $1 = e^{-i2M\theta}$. If $\theta/\pi = n/m$ (with n, m being coprime), the dimension of the representation M needs to be a multiple of m. This constraint strictly prohibits a continuous change in the Hamiltonian in the adiabatic heuristic principle.

In this paper, this puzzle is resolved. Although the Hamiltonian is defined only for discrete values of θ and its dimension behaves wildly, the energy gap defined by a dense set of Hamiltonians is surprisingly smooth and finite. It justifies the adiabatic heuristic principle on a torus. We also find the generalized Streda formula to explain the wild behavior of the degeneracy in terms of the many-body Chern number.

III. MODEL

We consider the periodic system of anyons in the uniform magnetic field on a square lattice with $N_x \times N_y$ sites. The Hamiltonian is

$$H = t\sum_{\langle ij\rangle} e^{i\phi_{ij}}e^{i\theta_{ij}}c_i^\dagger c_j \otimes W^{(ij)} + V\sum_{\langle ij\rangle} n_i n_j \otimes \mathbf{1}_M, \tag{2}$$

where $n_i = c_i^\dagger c_i$ and $c_i^\dagger$ (c_i) is the creation (annihilation) operator of a hard-core boson on site i. The hard-core condition is necessary to ensure consistency with the braid group. The Peierls phase $e^{i\phi_{ij}}$ is specified by the string gauge [33] for the external magnetic field. The phase $e^{i\theta_{ij}}$ describes the statistical phase [29,30] (see the details below). $W^{(ij)}$ is an M-dimensional matrix [30] to ensure consistency with Eq. (1). When $\theta/\pi = n/m$, M is fixed to be m as the irreducible representation. We set $W^{(ij)} = W_x$ and W_y for (ij) describing

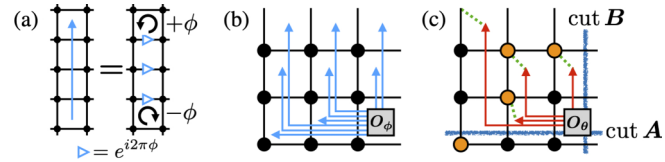

FIG. 2. (a) String gauge. Sketches of the 3×3 square lattice with (b) the string gauge ϕ_{ij} and (c) the statistical gauge θ_{ij}. The yellow points in (c) represent sites with anyons.

a pair of sites across the boundary in the x and y directions, respectively, and otherwise, $W^{(ij)} = \mathbf{1}_M$, where

$$W_x = \begin{bmatrix} 0 & 1 & \ldots & 0 \\ \vdots & \vdots & \ddots & \vdots \\ 0 & 0 & \ldots & 1 \\ e^{i\eta_x} & 0 & \ldots & 0 \end{bmatrix}, \tag{3}$$

$$W_y = e^{i\eta_y}\mathrm{diag}[e^{i2\theta}, e^{i4\theta}, \cdots, e^{i2M\theta}], \tag{4}$$

and $\vec{\eta} = (\eta_x, \eta_y)$ specifies the twisted boundary conditions. The Hamiltonian is consistent with Eq. (1) since we have $W_x^{-1}W_yW_xW_y^{-1} = e^{-i2\theta}\mathbf{1}_M$ for any $\vec{\eta}$.

Let us now give detailed descriptions of how to construct the Hamiltonian in Eq. (2). We first mention the string gauge ϕ_{ij} briefly. As shown in Fig. 2(a), let us consider a string on sites and assign the Peierls phase $e^{i2\pi\phi}$ on the links intersected by the string. They clearly describe the magnetic fluxes ϕ and $-\phi$ at the terminal and initial points of the string, respectively. Thus, the string gauge shown in Fig. 2(b) introduces the flux $\phi \times (1 - N_xN_y)$ to the plaquette with origin O_ϕ but introduces ϕ to the others. The gauge convention θ_{ij} is also described by the strings [see Fig. 2(c)]. The strings carry the phase factor $e^{i\theta}$, and their terminal points are located at plaquettes adjoining anyons. The additional rules are given as follows [30] (the roles of each rule are explained in Ref. [34]):

(i) If a string sweeps another anyon in the process of hopping, one determines the phase factor as if the anyon crosses the string.

(ii) When an anyon hops across cut B from left to right, the phase factor $e^{i(N_a-1)\theta}$ is given.

(iii) When an anyon hops across a horizontal string, the phase factor $e^{i2\theta}$, not $e^{i\theta}$, is given.

(iv) When an anyon hops across cut A upward, the phase factor $e^{iX\theta}$ is given, where X is the number of other anyons in the same x-axis position as the hopping anyon.

Due to Eqs. (3) and (4), we also give the following rules: When an anyon hops across cut B from left to right, the label is changed from w to $w - 1$, where w is the label of the basis $|\{\boldsymbol{r}_k\}; w\rangle$. If $w = 1$, the phase factor $e^{i\eta_x}$ is also given. Also, when an anyon hops across cut A upward, the phase factor $e^{i\eta_y}e^{i2w\theta}$ is given.

In this framework, the representations of the global move operators are given as $\tau_j = e^{i\frac{e}{\hbar}\alpha_j}e^{-i2\theta(j-1)}W_x$ and $\rho_j = e^{i\frac{e}{\hbar}\beta_j}e^{i2\theta(j-1)}W_y$, where $e^{i\frac{e}{\hbar}\alpha_j}$ and $e^{i\frac{e}{\hbar}\beta_j}$ are from the Peierls phase ϕ_{ij} describing the external magnetic field. As shown in Appendix A, these representations are consistent with the braid group on a torus.

The above construction of θ_{ij} introduces the magnetic flux $-2\pi \times 2\theta N_a$ only to the plaquette with origin O_θ shown

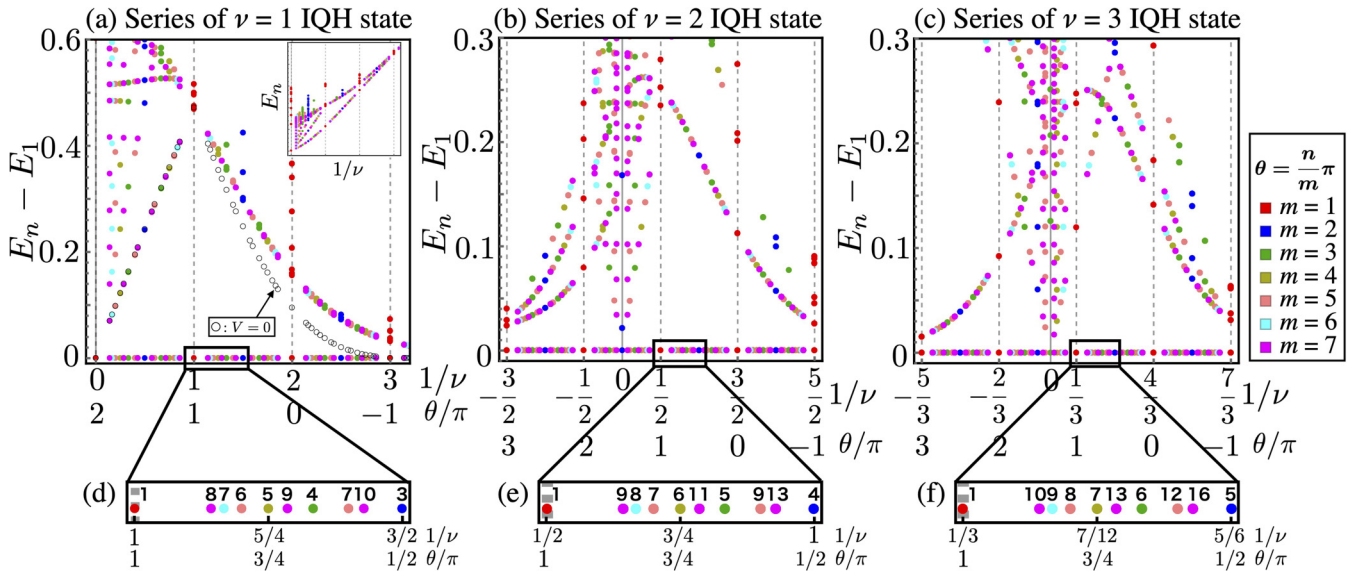

FIG. 3. (a)–(c) Energy gaps are shown as functions of $1/\nu$ for $t = -1$ and $V = 5$. The system size is $N_x \times N_y = 10 \times 10$. The statistical parameter θ is determined by $\nu = p/[p(1-\theta/\pi)+1]$ with (a) $p = 1$ (b) $p = 2$, and (c) $p = 3$. The vertical dashed lines represent $\theta/\pi =$ integer. The anyon number is (a) and (b) $N_a = 4$ and (c) $N_a = 3$. We plot the lowest $N_{\rm cut}$ states at each $1/\nu$ [$N_{\rm cut} = 40$ for (a) and (b) and $N_{\rm cut} = 70$ for (c)]. The open black circles in (a) are the gaps $E_{N_D+1} - E_1$ for $V = 0$. The inset in (a) is the energy spectrum with the same setting as in the main panel. (d)–(f) The ground-state degeneracy N_D is shown.

in Fig. 2(c) [30]. Since the string gauge ϕ_{ij} introduces the flux $\phi \times (1 - N_x N_y)$ to the plaquette with origin O_ϕ but ϕ to the others, as described above, one gets a condition of the uniformity of the magnetic field as $e^{i2\pi\phi(1-N_xN_y)-i2\theta N_a} = e^{i2\pi\phi}$. Since $N_\phi = \phi N_x N_y$, this condition is consistent with the relation $1/\nu + \theta/\pi = \text{const}$.

IV. ENERGY GAP

Using the above setup, we numerically diagonalize the Hamiltonians. In the following, we set $N_x = N_y = 10, t = -1$, $V = 5$, and $\vec{\eta} = \vec{0}$ unless otherwise stated. We assume that the states are degenerate if the energy difference is less than 0.001.

In Figs. 3(a)–3(c), we plot the energies of a series that includes the $\nu = p$ IQH state ($p = 1, 2, 3$) as a function of $1/\nu$. We show the data for $\theta = (n/m)\pi$ with various m and n ($m \leqslant 7$). The data points with different colors are eigenvalues of H with different dimensions. Figures 3(a)–3(c) show that the gap behaves smoothly for a dense set of Hamiltonians. The energies of the ground state are also smooth [see the inset in Fig. 3(a)].

Let us first consider a series of the $\nu = 1$ IQH state, which includes the Laughlin state. We here consider only $0 \leqslant \nu$ since a system of $\nu < 0$ is trivially mapped to that of $0 < \nu$. In Fig. 3(a), the threefold-degenerate ground state is obtained at $\nu = 1/3$, which is consistent with the lattice analog of the Laughlin state [35]. This state is adiabatically connected to the $\nu = 1$ IQH state. Note, however, that the ground-state degeneracy N_D changes wildly [see Fig. 3(d)]. At $1/\nu = 0$, the gap closing occurs, which suggests the Nambu-Goldstone modes associated with the superconductivity of hard-core bosons [36]. In Fig. 3(a), the results without the electron-electron interactions are also shown. While the ground states of anyons or bosons are gapped because of their hard-core nature, the gap at $\nu = 1/3$ vanishes since the system reduces to the partially filled lowest Landau band of free fermions. This implies that the interaction is crucially important only for the FQH states of fermions. In Fig. 4, the energy spectra as functions of the interaction V are shown. The FQH states remain gapped with the same topological degeneracy for a wide range of V apart from the point $V = 0$ in Fig. 4(c). Inclusion of the finite interaction V induces the gap at this point, which is consistent with the gapped Laughlin state. Although the discussion of the thermodynamic limit is an open question, our adiabatic heuristic argument for the fixed system size includes important scientific information.

As for the other series in Figs. 3(b) and 3(c), one can also see that the gaps remain open for each region $0 < 1/\nu$ and $1/\nu < 0$, although their topological degeneracy changes

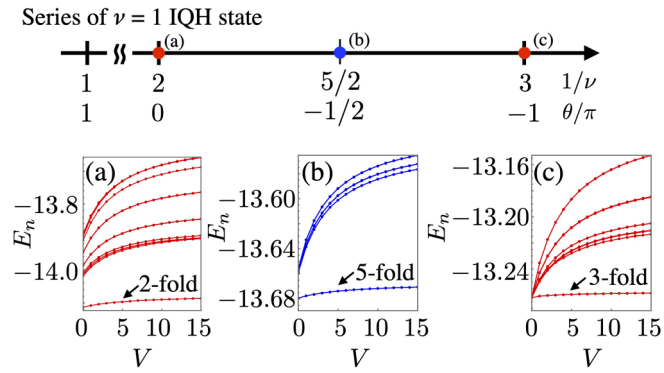

FIG. 4. Energy spectra are shown as functions of the interaction V for (a) the Boson FQH state at $\nu = 1/2$, (b) the anyon FQH state at $\nu = 2/5$, and (c) the Fermion FQH state at $\nu = 1/3$. They are included in a series of the $\nu = 1$ IQH state. We set $t = -1$ and $N_x \times N_y = 10 \times 10$. The lowest 40 states are shown in each panel.

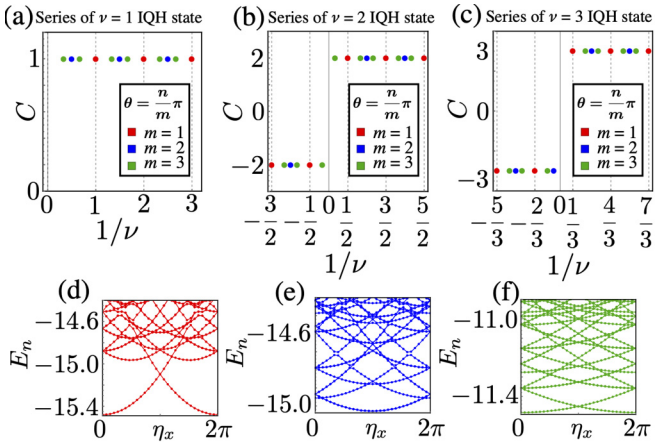

FIG. 5. (a)–(c) Chern number C of the degenerated ground-state multiplet is shown as a function of $1/\nu$. In (a), (b), and (c), we consider the systems in the same settings as in Figs. 3(a), 3(b) and 3(c), respectively. (d)–(f) Spectral flows at $1/\nu = 0$ for each series. We set $\eta_y = 0$. The statistics parameter is given by (d) $\theta/\pi = 2$, (e) $\theta/\pi = 3/2$, and (f) $\theta/\pi = 4/3$, respectively.

irregularly [see Figs. 3(e) and 3(f)]. The excitation gap closes at $1/\nu = 0$ in both figures, which is consistent with the emergence of the anyon superconductivity [37–39] of $\theta = (3/2)\pi$ and $\theta = (4/3)\pi$, respectively.

The numerical results in Fig. 3 suggest that the adiabatic heuristic principle remains valid for a series that includes the $\nu = p$ IQH state for the general integer p. It also suggests the realization of the anyon superconductivity of $\theta = (1 + 1/p)\pi$ by trading all the external magnetic fluxes for the statistical one.

Since $1/\nu \propto \phi$, where $\phi = N_\phi/(N_x N_y)$ is the number of fluxes per plaquette, this unusual but adiabatic behavior, in the sense that the gap remains open, is similar to the Azbel-Hofstadter problem [40–42] for the weak magnetic field limit. It implies that the adiabatic invariant of the evolution can be given by the Chern number of the ground-state multiplet. This is correct, as we discuss below.

V. ADIABATIC INVARIANT

As for the gapped ground-state multiplet of anyons, we calculate the many-body Chern number [5]

$$C = \frac{1}{2\pi i}\int_{T^2} d^2\eta F, \tag{5}$$

where $T^2 = [0, 2\pi] \times [0, 2\pi]$, $F = (\partial A_y/\partial\eta_x) - (\partial A_x/\partial\eta_y)$, $A_{x(y)} = \mathrm{Tr}\,[\Phi^\dagger(\partial\Phi/\partial\eta_{x(y)})]$, and $\Phi = (|G_1\rangle \cdots, |G_{N_D}\rangle)$ is a ground-state multiplet. In the numerical calculation, we use the method proposed in Ref. [43]. In Figs. 5(a)–5(c), we plot C for systems with the same settings as in Figs. 3(a)–3(c). Although the dimensions of the multiplet change wildly, the Chern number C remains the same. It suggests that C is an adiabatic invariant of the evolution. As for a series that includes the $\nu = p$ IQH state, we numerically obtain

$$C = \mathrm{sgn}(\nu) \times p, \tag{6}$$

where $\mathrm{sgn}(x)$ is the sign function. For $\nu > 0$, Eq. (6) is natural since the $\nu = p$ IQH state is included. However, the case with $\nu < 0$ is nontrivial since it does not include any simple state.

While the energy of the QH systems is almost independent of $\vec{\eta}$, the spectral flows at $1/\nu = 0$ exhibit strong $\vec{\eta}$ dependences [see Figs. 5(d)–5(f)]. They indicate the absence of the energy gap at $1/\nu = 0$, which implies the Nambu-Goldstone modes of the anyon superconductors.

VI. TOPOLOGICAL DEGENERACY

As mentioned above, the ground-state degeneracy changes wildly during the evolution, as shown in Figs. 3(d)–3(f). The fermion FQH state at $\nu = p/q$ is q-fold degenerate [44], but this pattern does not hold in the anyonic systems; the QH state with $(\nu, \theta/\pi) = (1, 1/2)$ in Fig. 3(e), for example, has fourfold degeneracy. We address this issue analytically below.

Let us consider a continuous translationally invariant system of size $L_x \times L_y$ with external magnetic field $B = \phi_0 N_\phi/(L_x L_y)$. The results obtained below are valid even for lattice models as long as ϕ is sufficiently small, i.e., the magnetic length becomes much larger than the lattice constant. The statistics of anyons is set as $\theta = (n/m)\pi$, and a translation operator of the center of mass is given by $T(\boldsymbol{a}) = \exp\{(i/\hbar)\sum_i \boldsymbol{K}_i \cdot \boldsymbol{a}\}$, where $\boldsymbol{K}_i = \boldsymbol{p}_i + e\boldsymbol{A}(\boldsymbol{r}_i) - eB\boldsymbol{e}_z \times \boldsymbol{r}_i$ [44–46]. Since the interactions of the system including the statistical vector potential [21] are given by the relative coordinates of anyons, $T(\boldsymbol{a})$ commutes with the Hamiltonian H. Noting that $T(\boldsymbol{b})^{-1}T(\boldsymbol{a})^{-1}T(\boldsymbol{b})T(\boldsymbol{a}) = e^{i\frac{e}{\hbar}B(\boldsymbol{a}\times\boldsymbol{b})N_a}$, let us now assume the following:

$$\rho_i^{-1}T(\boldsymbol{a})^{-1}\rho_i T(\boldsymbol{a}) = e^{i\frac{e}{\hbar}B(\boldsymbol{a}\times L_y\boldsymbol{e}_y)}, \tag{7}$$

$$T(\boldsymbol{b})^{-1}\tau_i^{-1}T(\boldsymbol{b})\tau_i = e^{i\frac{e}{\hbar}B(L_x\boldsymbol{e}_x\times\boldsymbol{b})} \tag{8}$$

since each loop given by Eqs. (7) and (8) does not enclose the other anyons.

Equation (1) implies $[\tau_i^m, \rho_j] = 0$. (The proof for any i and j is given in Appendix A.) Then by defining $\mathcal{T}_A \equiv T(\frac{1}{m}\frac{L_y}{N_\phi}\boldsymbol{e}_y)$, which satisfies

$$[\mathcal{T}_A, \tau_i^m] = [\mathcal{T}_A, \rho_i] = 0, \tag{9}$$

let us take the simultaneous eigenstate $|\psi_0\rangle$, which satisfies $H(\vec{\eta})|\psi_0\rangle = E(\vec{\eta})|\psi_0\rangle$ and $\mathcal{T}_A|\psi_0\rangle = e^{i\lambda}|\psi_0\rangle$ with λ being real. Here, the twisted boundary angles $\vec{\eta}$ are specified by τ_i^m and ρ_i with Eqs. (3) and (4). Further defining $\mathcal{T}_B \equiv T(\frac{L_x}{N_\phi}\boldsymbol{e}_x)$ and $\mathcal{T}_C \equiv \tau_1 T(\frac{n}{m}\frac{L_x}{N_\phi}\boldsymbol{e}_x)$, we define a new state $|\psi_{s,t}\rangle \equiv \mathcal{T}_B^s\mathcal{T}_C^t|\psi_0\rangle$. While $\mathcal{T}_B$ and $\mathcal{T}_C$ commute with τ_i^m and ρ_i, we have

$$\mathcal{T}_A\mathcal{T}_B = \mathcal{T}_B\mathcal{T}_A e^{i2\pi\frac{1}{m}\nu}, \tag{10}$$

$$\mathcal{T}_A\mathcal{T}_C = \mathcal{T}_C\mathcal{T}_A e^{i2\pi(\frac{1}{m}+\nu\frac{n}{m^2})}. \tag{11}$$

This implies $H(\vec{\eta})|\psi_{s,t}\rangle = E(\vec{\eta})|\psi_{s,t}\rangle$ and $\mathcal{T}_A|\psi_{s,t}\rangle = e^{i\lambda}e^{i2\pi f_{s,t}}|\psi_{s,t}\rangle$, with

$$f_{s,t} = \frac{\nu s + (1 + \nu\theta/\pi)t}{m} = \frac{\nu}{pm}[p(s+t) + t], \tag{12}$$

where $\nu = p/[p(1 - \theta/\pi) + 1]$ is used in the last part. Thus, the topological degeneracy N_{TD} is given by the number of

pairs (s,t) that give different values of $f_{s,t}$ mod 1. Since pm/ν is always an integer, one obtains $N_{\rm TD} = pm/|\nu|$. Using Eq. (6) and $M = m$ (irreducible representation), we have

$$N_{\rm TD} = MC/\nu. \tag{13}$$

This is consistent with the obtained ground-state degeneracy shown in Figs. 3(d)–3(f). The anyon nature shown in Eq. (11) gives the extra degeneracy compared with the fermionic standard case [44].

VII. GENERALIZED STREDA FORMULA

Taking the difference of Eq. (13) for two possible cases in a series, one obtains $\Delta N_{\rm TD}/\Delta(M/\nu) = C$, where we assume the Chern number C is the invariant. Since $M/\nu = MN_xN_y\phi/N_a$, with ϕ being the number of fluxes per plaquette, we finally have

$$\frac{\Delta(N_p/N'_{\rm site})}{\Delta\phi} = C, \tag{14}$$

where $N_p \equiv N_{\rm TD}N_a$ is the "parton" number corrected by the topological degeneracy and $N'_{\rm site} \equiv MN_xN_y$ is the extended number of sites due to the non-Abelian nature of the representation. This is a *generalized* Streda formula for anyons. Note that Eq. (14) for fermions ($M = 1$, $\nu = p/q$, $N_{\rm TD} = q$, $C = p$) reduces to the standard Streda formula [47]. When one includes a reducible representation of the braid group, i.e., $M = tm$, with $2 \leqslant t$ (t is an integer), the degeneracy $N_{\rm TD}$ increases t times. Therefore, Eqs. (13) and (14) hold generally.

VIII. CONCLUSION

In this paper, the adiabatic heuristic principle for the QH states was demonstrated on a torus numerically. The emergence of the anyon superconducting states was also suggested. The Chern number of the ground-state multiplet served as the adiabatic invariant of the evolution although its degeneracy changes wildly. The anyon nature brings the extra multiplicity to the topological degeneracy. It results in a generalized Streda formula that follows from the translational invariance. Extensions of this adiabatic principle on a torus could be useful to characterize the non-Abelian FQH states.

ACKNOWLEDGMENTS

We thank the Supercomputer Center, the Institute for Solid State Physics, University of Tokyo for the use of the facilities. The work is supported in part by JSPS KAKENHI Grants No. JP17H06138 (K.K., Y.H.) and No. JP19J12317 (K.K.).

APPENDIX A: CONSTRAINTS ON STATISTICAL PHASE

In this Appendix, we derive the relation $1/\nu + \theta/\pi =$ const from the braid group analysis on a torus. A proof of $[\tau_i^m, \rho_j] = 0$ for any i and j is also given here.

In the main text, we denote the generators of the braid group on a torus by σ_i, τ_i, and ρ_i. They satisfy the following relations [13,31,32]:

$$\tau_{i+1}^{-1}\rho_i\tau_{i+1}\rho_i^{-1} = (\sigma_i^{-1})^2, \tag{A1}$$

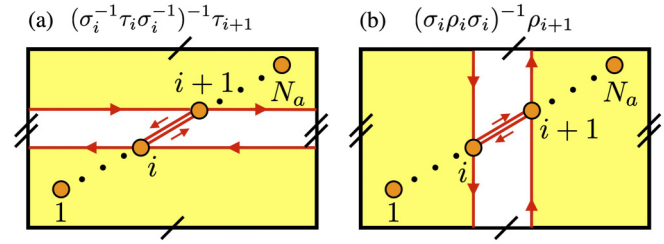

FIG. 6. Closed paths defined by (a) $(\sigma_i^{-1}\tau_i\sigma_i^{-1})^{-1}\tau_{i+1}$ and (b) $(\sigma_i\rho_i\sigma_i)^{-1}\rho_{i+1}$.

$$\rho_1^{-1}\tau_1^{-1}\rho_1\tau_1 = \sigma_1\cdots\sigma_{N_a-1}\sigma_{N_a-1}\cdots\sigma_1 e^{i\frac{e}{\hbar}BL_xL_y}, \tag{A2}$$

$$\tau_{i+1} = \sigma_i^{-1}\tau_i\sigma_i^{-1}e^{i\frac{e}{\hbar}(\alpha_{i+1}-\alpha_i)}, \tag{A3}$$

$$\rho_{i+1} = \sigma_i\rho_i\sigma_i e^{i\frac{e}{\hbar}(\beta_{i+1}-\beta_i)}, \tag{A4}$$

where α_i and β_i are real numbers. Equation (A1) is the same as Eq. (1). The derivations of Eqs. (A3) and (A4) are given in Appendix B.

Substituting $\sigma_i = e^{i\theta}\mathbf{1}_M$ into Eqs. (A1), (A2), (A3), and (A4), we have

$$\rho_i\tau_{i+1} = \tau_{i+1}\rho_i e^{-i2\theta}, \tag{A5}$$

$$\rho_1\tau_1 = \tau_1\rho_1 e^{i2(N_a-1)\theta+i2\pi N_\phi}, \tag{A6}$$

$$\tau_{i+1} = \tau_i e^{-i2\theta}e^{i\frac{e}{\hbar}(\alpha_{i+1}-\alpha_i)}, \tag{A7}$$

$$\rho_{i+1} = \rho_i e^{i2\theta}e^{i\frac{e}{\hbar}(\beta_{i+1}-\beta_i)}. \tag{A8}$$

Here, we note that the representations

$$\tau_j = e^{i\frac{e}{\hbar}\alpha_j}e^{-i2\theta(j-1)}W_x, \tag{A9}$$

$$\rho_j = e^{i\frac{e}{\hbar}\beta_j}e^{i2\theta(j-1)}W_y \tag{A10}$$

satisfy the relations in Eqs. (A5), (A6), (A7), and (A8). Substituting Eq. (A7) into Eq. (A5), one gets

$$\rho_i\tau_j = \tau_j\rho_i e^{-i2\theta}. \tag{A11}$$

If $\theta/\pi = n/m$, it reduces to $[\tau_i^m, \rho_j] = 0$. Comparing Eq. (A11) for $i = j = 1$ with Eq. (A6), we get

$$e^{i2\theta N_a + i2\pi N_\phi} = 1. \tag{A12}$$

This implies that $\theta/\pi + 1/\nu = 2\pi s/N_a$, with s being an integer.

APPENDIX B: NONCONTRACTIBLE LOOPS ON A TORUS

In this Appendix, we prove Eqs. (A3) and (A4). If the magnetic flux is absent, the relations of the braid group are given as [13,28]

$$\tau_{i+1} = \sigma_i^{-1}\tau_i\sigma_i^{-1}, \tag{B1}$$

$$\rho_{i+1} = \sigma_i\rho_i\sigma_i. \tag{B2}$$

Note that $(\sigma_i^{-1}\tau_i\sigma_i^{-1})^{-1}\tau_{i+1}$ and $(\sigma_i\rho_i\sigma_i)^{-1}\rho_{i+1}$ move anyons along closed loops shown in Figs. 6(a) and 6(b), respectively.

Therefore, if the magnetic field described by the vector potential $\boldsymbol{A}(\boldsymbol{r})$ is present, $(\alpha_{i+1}-\alpha_i)/\phi_0$ and $(\beta_{i+1}-\beta_i)/\phi_0$ fluxes penetrate each closed path, respectively, where $\alpha_i = \oint_{L_{\tau_i}} d\boldsymbol{r}\cdot\boldsymbol{A}(\boldsymbol{r})$, $\beta_i = \oint_{L_{\rho_i}} d\boldsymbol{r}\cdot\boldsymbol{A}(\boldsymbol{r})$, and $L_{\tau_i(\rho_i)}$ is the path given by $\tau_i(\rho_i)$. Then we obtain Eqs. (A3) and (A4).

[1] K. v. Klitzing, G. Dorda, and M. Pepper, Phys. Rev. Lett. **45**, 494 (1980).
[2] D. C. Tsui, H. L. Stormer, and A. C. Gossard, Phys. Rev. Lett. **48**, 1559 (1982).
[3] D. J. Thouless, M. Kohmoto, M. P. Nightingale, and M. den Nijs, Phys. Rev. Lett. **49**, 405 (1982).
[4] M. Kohmoto, Ann. Phys. (NY) **160**, 343 (1985).
[5] Q. Niu, D. J. Thouless, and Y.-S. Wu, Phys. Rev. B **31**, 3372 (1985).
[6] M. V. Berry, Proc. R. Soc. London, Ser. A **392**, 45 (1984).
[7] R. B. Laughlin, Phys. Rev. Lett. **50**, 1395 (1983).
[8] X. G. Wen, Phys. Rev. B **40**, 7387 (1989).
[9] D. Arovas, J. R. Schrieffer, and F. Wilczek, Phys. Rev. Lett. **53**, 722 (1984).
[10] F. D. M. Haldane, Phys. Rev. Lett. **51**, 605 (1983).
[11] B. I. Halperin, Phys. Rev. Lett. **52**, 1583 (1984).
[12] X.-G. Wen, Adv. Phys. **44**, 405 (1995).
[13] T. Einarsson, Phys. Rev. Lett. **64**, 1995 (1990).
[14] M. Oshikawa and T. Senthil, Phys. Rev. Lett. **96**, 060601 (2006).
[15] M. Sato, M. Kohmoto, and Y.-S. Wu, Phys. Rev. Lett. **97**, 010601 (2006).
[16] R. Willett, J. P. Eisenstein, H. L. Störmer, D. C. Tsui, A. C. Gossard, and J. H. English, Phys. Rev. Lett. **59**, 1776 (1987).
[17] G. Moore and N. Read, Nucl. Phys. B **360**, 362 (1991).
[18] N. Read and E. Rezayi, Phys. Rev. B **59**, 8084 (1999).
[19] A. Kitaev, Ann. Phys. (NY) **303**, 2 (2003).
[20] C. Nayak, S. H. Simon, A. Stern, M. Freedman, and S. Das Sarma, Rev. Mod. Phys. **80**, 1083 (2008).
[21] F. Wilczek, Phys. Rev. Lett. **49**, 957 (1982).
[22] J. K. Jain, Phys. Rev. Lett. **63**, 199 (1989).
[23] J. K. Jain, *Composite Fermions* (Cambridge University Press, Cambridge, 2007).
[24] M. Greiter and F. Wilczek, Mod. Phys. Lett. B **04**, 1063 (1990).
[25] M. Greiter and F. Wilczek, Nucl. Phys. B **370**, 577 (1992).
[26] Y.-S. Wu, Phys. Rev. Lett. **52**, 2103 (1984).
[27] Since the system of anyons is intrinsically a many-body problem, the construction of the pseudopotential projected into the lowest Landau level is impossible. Therefore, we choose a toroidal lattice model for the direct numerical demonstrations. This geometry is also suitable for evaluation of the topological numbers.
[28] J. S. Birman, Commun. Pure Appl. Math. **22**, 41 (1969).
[29] X. G. Wen, E. Dagotto, and E. Fradkin, Phys. Rev. B **42**, 6110 (1990).
[30] Y. Hatsugai, M. Kohmoto, and Y.-S. Wu, Phys. Rev. B **43**, 10761 (1991).
[31] T. Einarsson, Mod. Phys. Lett. B **05**, 675 (1991).
[32] D. Li, Int. J. Mod. Phys. B **07**, 2779 (1993).
[33] Y. Hatsugai, K. Ishibashi, and Y. Morita, Phys. Rev. Lett. **83**, 2246 (1999).
[34] Rule (i) ensures the local exchange operation. Rules (ii) and (iii) remove the artificial twisted boundary condition in the x and y directions caused by anyon fluxes, respectively. The necessity of rule (iv) comes from ordering vertical anyon strings of particles in the same x-axis position as the hopping anyon.
[35] K. Kudo, T. Kariyado, and Y. Hatsugai, J. Phys. Soc. Jpn. **86**, 103701 (2017).
[36] S. C. Zhang, Int. J. Mod. Phys. B **06**, 25 (1992).
[37] R. B. Laughlin, Phys. Rev. Lett. **60**, 2677 (1988).
[38] A. L. Fetter, C. B. Hanna, and R. B. Laughlin, Phys. Rev. B **39**, 9679 (1989).
[39] Y.-H. Chen, F. Wilczek, E. Witten, and B. I. Halperin, Int. J. Mod. Phys. B **03**, 1001 (1989).
[40] M. Y. Azbel, Zh. Eksp. Teor. Fiz. **46**, 929 (1964) [J. Exp. Theor. Phys. **19**, 634 (1964)].
[41] D. R. Hofstadter, Phys. Rev. B **14**, 2239 (1976).
[42] Y. Hasegawa, Y. Hatsugai, M. Kohmoto, and G. Montambaux, Phys. Rev. B **41**, 9174 (1990).
[43] T. Fukui, Y. Hatsugai, and H. Suzuki, J. Phys. Soc. Jpn. **74**, 1674 (2005).
[44] F. D. M. Haldane, Phys. Rev. Lett. **55**, 2095 (1985).
[45] J. Zak, Phys. Rev. **134**, A1602 (1964).
[46] R. Tao and F. D. M. Haldane, Phys. Rev. B **33**, 3844 (1986).
[47] P. Streda, J. Phys. C **15**, L717 (1982).